Astrometric Measurements of the Double Star Systems AG 85, STF 414, and STI 2036

Thomas Morford[1], Sabine Mazzeo[1], Jacob Bryant[1], and Kalée Tock[1]
[1]Stanford Online High School, Redwood City, California; agent07@ohs.stanford.edu

Abstract

The double star systems WDS 05024+0419 (AG 85), WDS 03345+1948 (STF 414), and WDS 04105+5717 (STI 2036) were measured astrometrically for inclusion in the Washington Double Star Catalog. Ten images of each system were reduced to obtain the position angle (θ) and separation (ρ) of the two stars. These measurements were then analyzed alongside information from the Gaia Data Release 3 (GDR3) and historical data from the US Naval Observatory to investigate the relationship between each pair of stars. It was concluded that all three systems are unlikely to be gravitationally bound because their relative velocities exceed their corresponding system escape velocities by more than two orders of magnitude, and the systems have significant separation in the radial dimension. However, all three systems do exhibit comparable proper motion (PM), suggesting that their stars are physically linked.

1. Introduction

To choose the double star systems for this study, the following constraints were input into Stelle Doppie, an online catalog for double star systems:

Each system must have a right ascension (RA) between 3 and 13 hours, so that they were visible in January when this study was conducted. The declination (DEC) of the systems was not a concern as the Las Cumbres Observatory Global Telescope (LCOGT) network that we used includes telescopes in both hemispheres (T. M. Brown et al. 2013).

The systems should each have a ρ greater than $5''$ to ensure that the images (taken by 0.4 m telescopes) distinctly show both stars. It should also be less than $20''$ to increase the chance that the physical relationship between the stars would be apparent from the historical data. A greater ρ corresponds to a longer orbital period for gravitationally bound systems, so for these widely-separated systems, the historical data will generally have little indication of binary stars' orbits, since the data only goes back a few centuries.

The final constraint is that the secondary star should be brighter than 13 (magnitude < 13) to be easily visible with the LCOGT 0.4 m instruments, and the difference in magnitude between the two stars (Δ mag) should be less than 3. A Δ mag greater than 3 would reduce the number of exposure times for which both stars are clearly visible.

The systems AG 85, STF 414, and STI 2036 were chosen. The stars' θ and ρ values (calculated from the individual GDR3 star coordinates) are presented along with other relevant data from GDR3 in Table 1 (Gaia Collaboration, Prusti, et al. 2016; Gaia Collaboration, A. G. A. Brown, et al. 2021).

Table 1: Information about the systems.

System	Constellation	Coordinates	Exposure times (s)	θ (°)	ρ (″)	Primary Gmag	Secondary Gmag	Δ Gmag
AG 85	Orion	$5\,\mathrm{h}\,2'\,24.67''$ $+4°\,19'\,23.7''$	5.90	176.2	9.42	9.544	10.311	0.767
STF 414	Taurus	$3\,\mathrm{h}\,34'\,27.73''$ $+19°\,47'\,52.4''$	1.09	185.8	7.51	8.116	8.256	0.140
STI 2036	Camelopardalis	$4\,\mathrm{h}\,10'\,27.5''$ $+57°\,15'\,47.3''$	8.75	55.2	8.80	10.225	10.686	0.461

2. Instruments Used

The images were taken using LCOGT $0.4\,\mathrm{m}$ Aqawan A telescopes in Cerro Tololo, Chile and in Tenerife, Spain. The telescopes are equipped with an SBIG STL6303 camera with a field of view of $29.2'' \times 19.5''$ and a pixel size of $0.571''$/pixel. They have a Meade 16-inch Robotic Control System (RCS) tube and 3-element optics. The images were calibrated with the LCO pipeline (T. M. Brown et al. 2013), and then taken with their Pan-STARRS w filter. The exposure times used for each star are listed in Table 1 above.

3. Measurements

All 10 of the images requested from LCOGT—taken over the period of one night—for each system came back clearly resolving both stars of each pair. The images were then reduced using the AstroImageJ software, whose multi-aperture photometry tool was used to find the θ and ρ of the stars. An appropriate aperture size was chosen for each pair, as shown in Section 3. The apertures that covered the stars' full diameters without overlapping are as follows: $6''$ for AG 85, $4''$ for STF 414, and $4.6''$ for STI 2036.

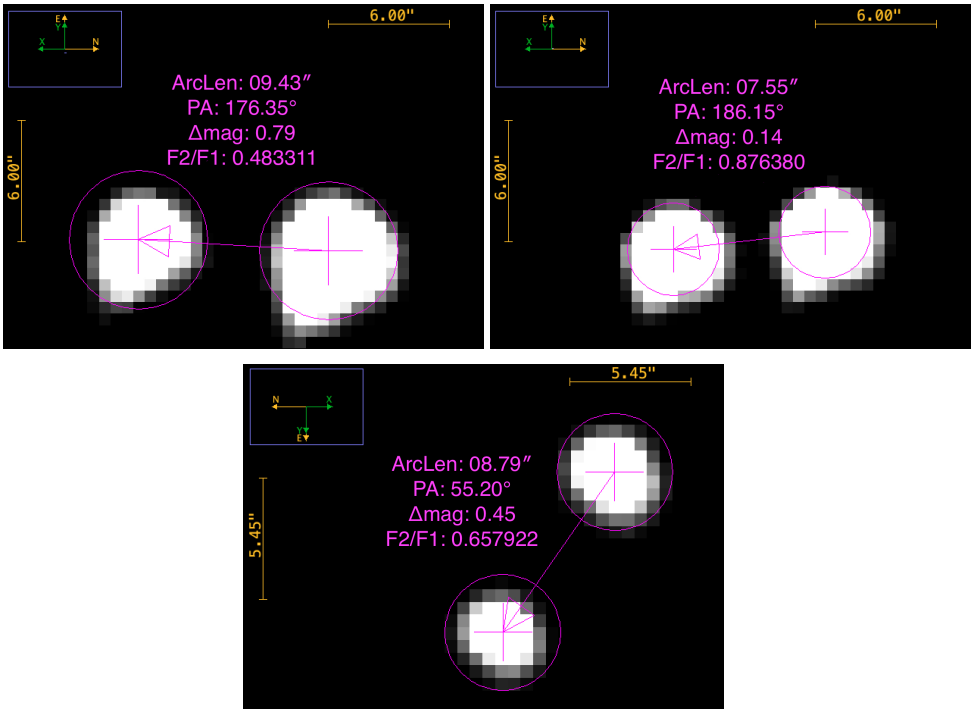

Figure 1: Measuring the systems' θ and ρ in the AstroImageJ program (from left to right: AG 85, STF 414, and STI 2036)

AstroImageJ finds the center of the star by locating the pixel whose brightness equals the weighted average brightness of all the pixels in the aperture. It uses this to determine the stars' θ and ρ values, recorded in Table 2. The averages of these measurements, listed in the last row of the table, serve as estimates of the current θ and ρ of the systems. The Δ mag between the two stars in each system is included as a reference for future studies. It is worth noting that the Δ mags of STF 414 seem irregular, making it a potential candidate for followup photometric analysis.

Table 2: θ and ρ of each measured image.

AG 85			STF 414			STI 2036		
θ	ρ	Δ mag	θ	ρ	Δ mag	θ	ρ	Δ mag
176.4	9.43	0.789	186.2	7.55	0.143	55.2	8.79	0.455
176.3	9.42	0.794	185.8	7.56	0.147	55.0	8.80	0.457
176.2	9.42	0.786	185.6	7.56	0.162	55.0	8.80	0.449
176.3	9.39	0.796	186.1	7.52	0.188	55.2	8.79	0.452
176.2	9.41	0.792	186.2	7.59	0.142	55.1	8.79	0.460
176.2	9.39	0.796	186.2	7.52	0.133	55.1	8.81	0.457
176.4	9.45	0.791	185.2	7.49	0.158	55.2	8.78	0.454
176.2	9.40	0.795	185.4	7.53	0.132	55.3	8.78	0.452
176.3	9.39	0.797	185.6	7.59	0.117	55.0	8.76	0.455
176.2	9.42	0.793	186.1	7.48	0.135	55.1	8.79	0.445
176.3	9.41	0.793	186.0	7.54	0.146	55.1	8.79	0.454

4. Analysis

In order to estimate the masses of the stars, which is essential to the escape velocity calculation later in Table 7, the distance to the star is needed. There are a few possible sources for distance—a brief discussion and summary of these values follows. GDR3 provides both distance measurements, calculated from the "GSP-Phot Aeneas best library using BP/RP spectra" (Gaia Collaboration, Prusti, et al. 2016; Gaia Collaboration, A. G. A. Brown, et al. 2021), and parallax measurements, which can be inverted to find the distance. Cruzalèbes et al. 2019 also estimates the distance from Gaia Data Release 2 (GDR2) data. There are minor discrepancies among all of these values, as shown in Table 3. We have chosen to use GDR3 as it is more recent than Cruzalèbes et al. 2019, and since GDR3 is a standard source, we will rely on its reduced distance value rather than calculating the distance by inverting the parallax.

Table 3: Distance measurements and estimates.

Star	GDR3 parallax (mas)	Cruzalèbes et al. 2019 distance (pc)	GDR3 distance (pc)	Distance from parallax (pc)
AG 85 Primary	3.89 ± 0.017	263.9	255.1	256.8
AG 85 Secondary	4.30 ± 0.046	–	244.8	232.8
STF 414 Primary	2.73 ± 0.129	499.6	250.5	366.1
STF 414 Secondary	3.02 ± 0.041	325.7	378.0	331.6
STI 2036 Primary	1.35 ± 0.014	795.1	740.0	740.0
STI 2036 Secondary	1.38 ± 0.015	728.0	778.8	726.6

We use Eq. (1) (whose derivation and geometric explanation is shown in Appendix A) to calculate and check the stellar radii of the targets against what is given by GDR3, which provides a stellar radius, though not an

angular radius, via its "Astrophysical Parameters" table. This estimate provides a value for all of our target stars except AG 85's secondary star, for which an angular diameter is not given in GDR2 (nor in GDR3, which does not provide angular diameters). Since GDR3, the preferred source when available, does not list a stellar radius for STI 2036's primary star, this calculation was used as the primary source for that star's radius. The radii from GDR3 and from our calculations are displayed in Table 4. It is worth noting that in the case of STF 414, the radius of the primary is less than that of the secondary: the secondary star is in fact bigger and brighter than the primary star for this system.

$$\text{radius}_{R_\odot} = \frac{1}{2} \times \text{distance}_{pc} \times \text{angular diameter}_{mas} \times \frac{1'}{1000\,\text{mas}} \times \frac{1^\circ}{3600\,\text{mas}} \times \frac{\pi}{180^\circ} \times \frac{206\,265\,\text{au}}{1\,\text{pc}} \times \frac{215\,R_\odot}{1\,\text{au}} \quad (1)$$

Table 4: Radii and related values.

Star	Cruzalèbes et al. 2019 angular diameter (mas)	Calculated stellar radius ($R_\odot$)	GDR3 stellar radius ($R_\odot$)
AG 85 Primary	0.07	1.9	2.0
AG 85 Secondary	–	–	1.5
STF 414 Primary	0.13	3.5	2.4
STF 414 Secondary	0.14	5.6	3.3
STI 2036 Primary	0.08	6.1	–
STI 2036 Secondary	0.06	4.9	4.0

The masses and spectral types of the stars were queried from the GDR3 "Astrophysical Parameters" table, and listed in Table 5. The data for STI 2036 is incomplete, so spectral types were also collected from Cruzalèbes et al. 2019, who calculated them from the GDR2. STI 2036's spectral types were used to estimate its stars' masses according to the mass-luminosity relation (Morgan 2023). The large discrepancies between the GDR3 mass and estimated mass for AG 85 and STF 414 indicate the uncertainty in our estimates, so STI 2036's estimated mass should [be taken with a grain of salt]; the spectral types from both GDR3 Teff and Cruzalèbes et al. 2019 rely on estimates and inferences, hence the discrepancy shown in Table 5.

Table 5: Information about the stars in each system.

Star	GDR3 spectral type	Cruzalèbes et al. 2019 spectral type	GDR3 mass	Mass estimated from Cruzalèbes et al. 2019
AG 85 Primary	F	A4/5	1.548	1.8
AG 85 Secondary	F	–	1.314	–
STF 414 Primary	B	A0	2.917	2.2
STF 414 Secondary	B	A0	2.764	2.2
STI 2036 Primary	A	B9	–	2.8
STI 2036 Secondary	–	B9	–	2.8

5. Plots

None of the three systems have previous orbital or linear solutions in the Sixth Catalog of Orbits of Visual Binary Stars. However, the U.S. Naval Observatory has historical observations and measurements of them, which can help determine if two stars are gravitationally bound. Bound stars exhibit a curvature over time of the position of the secondary star, while stars that are not bound correspond to a scattering of points.

This historical data is graphed in Section 5. The points are colored by date; darker ones are more recent. The red points correspond to the measurements presented in this paper.

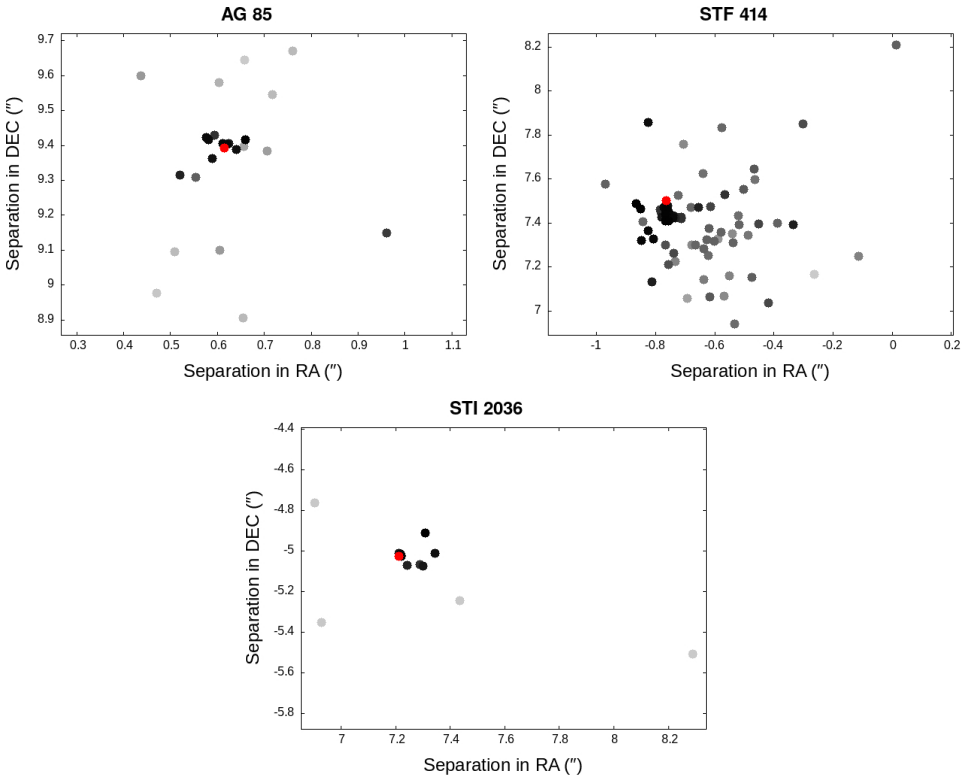

Figure 2: Historical data plots of AG 85, STF 414, and STI 2036

Based on these plots, none of the systems are likely to be gravitationally bound. The variability between the RA and DEC—and thus the θ and ρ—of the two stars decreases, rather than following a trend line, likely due to technological advancements enabling more accurate measurements. Also, the most recent measurements—including ours—are scattered throughout the graph among the earlier ones. This all suggests that the two stars in each system have been, and continue to be, moving in the same direction as each other, but are not gravitationally bound.

6. Results

Table 6 presents a summary of the image reduction described above. The averages of the θs and ρs in Table 2 from the 10 images taken of each system provide estimates of the stars' current θ and ρ. Additionally, the standard deviation and standard error are included as reinforcement of the steadiness of these measurements.

Table 6: The measured θ and ρ of each system.

System	Date	θ (°)	θ standard deviation	θ standard error	ρ (″)	ρ standard deviation	ρ standard error
AG 85	2023.0274	176.3	0.07	0.02	9.41	0.026	0.006
STF 414	2023.0164	185.8	0.37	0.12	7.54	0.038	0.012
STI 2036	2023.0164	55.1	0.16	0.03	8.79	0.014	0.004

Data about the stars' motions and escape velocity is displayed in Table 7.

It is important to consider is the stars' distances from Earth (listed in Table 3). Although the stars may have a small ρ, they could have a large radial separation (radial sep). The stars' radial sep is over 10 pc in all three systems, suggesting that they are too far apart from each other to be gravitationally bound.

The relative PM (rPM) metric is the magnitude of the difference vector for the two stars' PMs (the relative PM vector) divided by the longer PM vector (Harshaw 2016). A small rPM suggests that the two vectors do not separate as much when placed with their tails on the same origin, and thus have a similar direction of motion, which is a characteristic a gravitationally bound system would exhibit. An rPM that is less than 0.2 indicates common proper motion (CPM) as detailed by (Harshaw 2016). Both STF 414 and STI 2036 exhibit CPM. AG 85's rPM falls within the range that corresponds to similar proper motion (SPM)—that is, 0.2 < rPM < 0.6.

Escape velocity is another metric used to judge the likelihood of the systems being gravitationally bound. Using the estimated stellar masses in Table 5, the escape velocity for each gravitationally bound system with total mass M and radius r can be estimated using the equation $v_{\text{esc}} = \sqrt{\frac{2GM}{r}}$ (Bonifacio et al. 2020). None of the targets' parallax uncertainties overlap, so their three-dimensional separations were used to calculate their orbital radii r. The ratio between the resulting escape velocity and the three-dimensional relative velocity (3DRV) is over two orders of magnitude for each system, suggesting that the stars in each system would have too great a relative velocity to be held together in binary systems (Caputo et al. 2020).

Table 7: Calculated information about the systems.

System	Radial sep (pc)	Primary PM (mas/yr)	Secondary PM (mas/yr)	rPM	Escape velocity (m/s)	3DRV (m/s)
AG 85	24.0 ± 3.604	6.91 ± 0.018, 3.45 ± 0.014	4.22 ± 0.056, 7.92 ± 0.041	0.581	30	4000
STF 414	34.5 ± 21.787	-3.82 ± 0.159, -7.31 ± 0.106	-4.24 ± 0.051, -8.53 ± 0.032	0.135	30	7800
STI 2036	13.3 ± 15.561	-1.13 ± 0.015, -2.05 ± 0.012	-1.11 ± 0.016, -2.05 ± 0.013	0.012	60	7700

7. Conclusion

The measurements from the data reductions of each system fit well into the clump of historical data in the systems' respective graphs of RA versus DEC, implying both that the measurements are accurate and that the stars have not exhibited significant relative motion over the time they have been observed. This is further supported by the rPM of the systems, which categorizes AG 85 as having SPM and STF 414 and STI 2036 as having CPM. The historical data does not suggest any curvature but rather a lack of movement as we get to

more recent data points, suggesting that the two stars are moving alongside each other, rather than orbiting each other.

The parallax tells us that the radial sep is too great for the systems to be gravitationally bound. Additionally, for all three systems, the escape velocity is greater than the 3DRV, which means that the stars could not be held together in a system; they are moving too quickly for the limits of the potential binary system.

While it is unlikely for any of the three systems to be binary, the historical data and rPM of each pair of stars indicates that they are moving through space together. Thus it is plausible that AG 85, STF 414, and STI 2036 are all individually physically related pairs in the sense that they have comparable proper motion.

Acknowledgements

This research was made possible by the Washington Double Star catalog maintained by the U.S. Naval Observatory, the Stelle Doppie catalog maintained by Gianluca Sordiglioni, Astrometry.net, and the AstroImageJ software written by Karen Collins and John Kielkopf.

This work made use of Astropy:[1] a community-developed core Python package and an ecosystem of tools and resources for astronomy (Astropy Collaboration, Robitaille, et al. 2013; Astropy Collaboration, A. M. Price-Whelan, et al. 2018; Astropy Collaboration, Adrian M. Price-Whelan, et al. 2022).

Astroquery (Ginsburg et al. 2019), Matplotlib (Hunter 2007), and IPython (Pérez and Granger 2007) were used in the creation of the plots.

This work has also made use of data from the European Space Agency (ESA) mission Gaia (https://www.cosmos.esa.int/gaia), processed by the Gaia Data Processing and Analysis Consortium (DPAC, https://www.cosmos.esa.int/web/gaia/dpac/consortium). Funding for the DPAC has been provided by national institutions, in particular the institutions participating in the Gaia Multilateral Agreement.

This work makes use of observations taken by the 0.4 m telescopes of the Las Cumbres Observatory Global Telescope Network located in Cerro Tololo, Chile and Tenerife, Spain.

This research has made use of the SIMBAD database, operated at CDS, Strasbourg, France (Wenger et al. 2000).

We thank Thomas Smith for reviewing this paper.

References

Astropy Collaboration, A. M. Price-Whelan, et al. (Sept. 2018). "The Astropy Project: Building an Open-science Project and Status of the v2.0 Core Package". In: Astronomical Journal 156.3, 123, p. 123. DOI: 10.3847/1538-3881/aabc4f. arXiv: 1801.02634 [astro-ph.IM].

Astropy Collaboration, Adrian M. Price-Whelan, et al. (Aug. 2022). "The Astropy Project: Sustaining and Growing a Community-oriented Open-source Project and the Latest Major Release (v5.0) of the Core Package". In: *Astrophysical Journal* 935.2, 167, p. 167. DOI: 10.3847/1538-4357/ac7c74. arXiv: 2206.14220 [astro-ph.IM].

Astropy Collaboration, T. P. Robitaille, et al. (Oct. 2013). "Astropy: A community Python package for astronomy". In: Astronomy and Astrophysics 558, A33, A33. DOI: 10.1051/0004-6361/201322068. arXiv: 1307.6212 [astro-ph.IM].

[1] http://www.astropy.org

Bonifacio, B. et al. (Dec. 2020). "Measurements of Neglected Double Stars". In: Journal of the American Association of Variable Star Observers 48.2, p. 262. URL: https://app.aavso.org/jaavso/article/3673/.

Brown, T. M. et al. (Sept. 2013). "Las Cumbres Observatory Global Telescope Network". In: Publications of the Astronomical Society of the Pacific 125.931, p. 1031. DOI: 10.1086/673168. arXiv: 1305.2437 [astro-ph.IM].

Caputo, R. et al. (Apr. 2020). "Observation and Investigation of 14 Wide Common Proper Motion Doubles in the Washington Double Star Catalog". In: *Journal of Double Star Observations* 16.2, pp. 173–182. URL: http://www.jdso.org/volume16/number2/Caputo_173_182.pdf.

Cruzalèbes, P. et al. (Dec. 2019). "A catalogue of stellar diameters and fluxes for mid-infrared interferometry". In: Monthly Notices of the Royal Astronomical Society 490.3, pp. 3158–3176. DOI: 10.1093/mnras/stz2803. arXiv: 1910.00542 [astro-ph.SR].

Gaia Collaboration, A. G. A. Brown, et al. (May 2021). "Gaia Early Data Release 3. Summary of the contents and survey properties". In: Astronomy and Astrophysics 649, A1, A1. DOI: 10.1051/0004-6361/202039657. arXiv: 2012.01533 [astro-ph.GA].

Gaia Collaboration, T. Prusti, et al. (Nov. 2016). "The Gaia mission". In: Astronomy and Astrophysics 595, A1, A1. DOI: 10.1051/0004-6361/201629272. arXiv: 1609.04153 [astro-ph.IM].

Ginsburg, Adam et al. (Mar. 2019). "astroquery: An Astronomical Web-querying Package in Python". In: Astronomical Journal 157.3, 98, p. 98. DOI: 10.3847/1538-3881/aafc33. arXiv: 1901.04520 [astro-ph.IM].

Harshaw, Richard (Apr. 2016). "CCD Measurements of 141 Proper Motion Stars: The Autumn 2015 Observing Program at the Brilliant Sky Observatory, Part 3". In: *Journal of Double Star Observations* 12.4, pp. 394–399. URL: https://ui.adsabs.harvard.edu/abs/2016JDSO...12..394H.

Hunter, J. D. (2007). "Matplotlib: A 2D graphics environment". In: *Computing in Science & Engineering* 9.3, pp. 90–95. DOI: 10.1109/MCSE.2007.55.

Morgan, S. (Jan. 2023). *Spectral Type Characteristics*. URL: https://sites.uni.edu/morgans/astro/course/Notes/section2/spectralmasses.html.

Pérez, Fernando and Brian E. Granger (May 2007). "IPython: a System for Interactive Scientific Computing". In: *Computing in Science and Engineering* 9.3, pp. 21–29. ISSN: 1521-9615. DOI: 10.1109/MCSE.2007.53. URL: https://ipython.org.

Wenger, M. et al. (Apr. 2000). "The SIMBAD astronomical database. The CDS reference database for astronomical objects". In: Astronomy and Astrophysics Supplement 143, pp. 9–22. DOI: 10.1051/aas:2000332. arXiv: astro-ph/0002110 [astro-ph].

A. Appendix A

Equation (A1) shows an example calculation of the solar radius for AG 85, with a distance of 256 pc and an angular diameter of 0.068 mas.

$$265\,\mathrm{pc} \times 0.068\,\mathrm{mas} \times \frac{1'}{1000\,\mathrm{mas}} \times \frac{1^\circ}{3600'} \times \frac{\pi}{180^\circ} \times \frac{206\,265\,\mathrm{au}}{1\,\mathrm{pc}} \times \frac{215\,\mathrm{R}_\odot}{1\,\mathrm{au}} = 3.8\,\mathrm{R}_\odot \qquad \text{(A1)}$$

This formula is justified in Fig. A1 and Eq. A2-5, in which θ is the angular diameter, d is the distance of the star (given by the parallax), and r is the radius of the star (all of these values are from GDR3). From the small angle approximation, $\tan\left(\frac{1}{2}\theta\right) \approx \frac{1}{2}\theta$; this lack of precision is not a concern as the distance itself has some uncertainty.

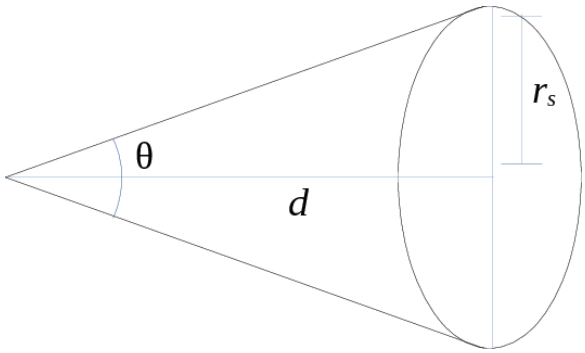

Figure A1: Geometric justification of Eq. (A1)

$$\tan\left(\frac{1}{2}\theta\right) = \frac{r_s}{d} \tag{A2}$$

$$r_s = d \times \tan\left(\frac{1}{2}\theta\right) \tag{A3}$$

$$r_s = d \times \frac{1}{2}\theta \tag{A4}$$

$$r_s = \frac{1}{2} \times d \times \theta \tag{A5}$$